

## Realistic quantum critical point in one-dimensional two-impurity models

Benedikt Lechtenberg,<sup>1,2,\*</sup> Fabian Eickhoff,<sup>1</sup> and Frithjof B. Anders<sup>1</sup>

<sup>1</sup>*Lehrstuhl für Theoretische Physik II, Technische Universität Dortmund, 44221 Dortmund, Germany*

<sup>2</sup>*Department of Physics, Kyoto University, Kyoto 606-8502, Japan*

(Received 30 September 2016; revised manuscript received 31 May 2017; published 7 July 2017)

We show that the two-impurity Anderson model exhibits an additional quantum critical point at infinitely many specific distances between both impurities for an inversion symmetric one-dimensional dispersion. Unlike the quantum critical point previously established, it is robust against particle-hole or parity symmetry breaking. The quantum critical point separates a spin doublet from a spin singlet ground state and is, therefore, protected. A finite single-particle tunneling  $t$  or an applied uniform gate voltage will drive the system across the quantum critical point. The discriminative magnetic properties of the different phases cause a jump in the spectral functions at low temperature, which might be useful for future spintronics devices. A local parity conservation will prevent the spin-spin correlation function from decaying to its equilibrium value after spin manipulations.

DOI: [10.1103/PhysRevB.96.041109](https://doi.org/10.1103/PhysRevB.96.041109)

**Introduction.** The promising perspective of combining traditional electronics with novel spintronics devices leads to intense research into controlling and switching the magnetic properties of such nanodevices. Experimentally magnetic properties of adatoms on surfaces [1–6] or magnetic molecules [7–14] might serve as the smallest building blocks for spintronic devices.

From a theoretical perspective, the two-impurity Anderson model (TIAM) [15–17] constitutes an important but simple system which embodies the competition of interactions between two localized magnetic moments with those between the impurities and the conduction band. The TIAM has been viewed as a paradigm model for the formation of two different singlet phases separated by a quantum critical point (QCP): a Ruderman-Kittel-Kasuya-Yosida (RKKY)-induced singlet and a Kondo singlet [15]. This QCP investigated by Jones and Varma [17–19], however, turned out to be unstable against particle-hole (PH) symmetry breaking [20] and the two different singlet phases are adiabatically connected. This led to the conclusion that for finite distances between the impurities, no QCP exists and the original finding is just a consequence of unphysical approximations [21] which is generically replaced by a crossover regime.

In this Rapid Communication, we establish that the model exhibits another realistic QCP for any inversion symmetric one-dimensional (1D) dispersion, depending only on the absolute value of the wave vector. The existence of this different QCP relies only on the fact that for specific distances  $R$  between both impurities, either the even- or odd-parity contributions to the conduction band decouple from the impurities at low-energy scales, leading to an underscreened Kondo effect. This underscreened Kondo fixed point (USK FP) [22] has a doublet ground state which is different from the singlet ground state for large antiferromagnetic interactions between both impurities, excluding a smooth crossover between both phases. This QCP trivially also exists for the limit  $R \rightarrow 0$  in all dimensions [23,24]: For this special case, the QCP has been recently observed in molecular dimers [7], where

the different phases can clearly be detected in the scanning tunneling spectra.

Here, we present the generalization to finite distances, its robustness against particle-hole symmetry as well as parity breaking, and demonstrate that the quantum phase transition (QPT) can also be evoked by applying a gate voltage to the impurities. Since the entanglement between the impurity spins is protected by a dynamical symmetry in the parity-symmetric case, the spin-spin correlation function cannot completely decay to its equilibrium value, and, therefore, might be useful for future qubit implementations. Possible experimental realizations for finite distances could be in pseudo-1D nanostructures [25–29] or optical lattices [30–32].

**Model.** We consider the two-impurity Anderson model (TIAM) whose Hamiltonian can be separated into the parts  $H_{\text{TIAM}} = H_c + H_D + H_I$ .  $H_c$  contains the conduction band  $H_c = \sum_{\vec{k},\sigma} \epsilon(\vec{k}) c_{\vec{k},\sigma}^\dagger c_{\vec{k},\sigma}$  and  $H_D$  and  $H_I$  comprise the impurity contribution and the interaction between the conduction band and impurities, respectively,

$$H_D = \sum_{j,\sigma} E_j d_{j,\sigma}^\dagger d_{j,\sigma} + U \sum_j n_{j,\uparrow} n_{j,\downarrow} + \vec{h} \sum_j \vec{S}_j + \frac{t}{2} \sum_{\sigma} (d_{1,\sigma}^\dagger d_{2,\sigma} + d_{2,\sigma}^\dagger d_{1,\sigma}), \quad (1)$$

$$H_I = \frac{V}{\sqrt{N}} \sum_{j \in \{1,2\}k,\sigma} c_{k,\sigma}^\dagger e^{ikR_j} d_{j,\sigma} + \text{H.c.}, \quad (2)$$

with  $d_{j,\sigma}^\dagger$  creating an electron with spin  $\sigma$  and energy  $E_j$  on impurity  $j$  located at position  $R_{1/2} = \pm R/2$ ,  $n_{j,\sigma} = d_{j,\sigma}^\dagger d_{j,\sigma}$ , a local magnetic field  $\vec{h}$  applied to the spin  $\vec{S}_j = \frac{1}{2} d_{j,\sigma}^\dagger \vec{\sigma}_{\sigma,\sigma'} d_{j,\sigma}$  of impurity  $j$ , and  $c_{k,\sigma}^\dagger$  creating a conduction electron. At low temperatures, the tunneling  $t$  leads to an effective antiferromagnetic exchange interaction  $K \vec{S}_1 \vec{S}_2$ , with  $K = t^2/U$  between the impurity spins. Throughout this work, unless stated otherwise, we will consider the case  $E_1 = E_2 = E = -U/2$  for simplicity such that both impurities are occupied with one electron. Below, we will show that the QCP is wholly robust to a departure from parity and particle-hole symmetries.

For the numerical renormalization-group (NRG) approach [33–36], it is useful to introduce a parity eigenbasis

\*benedikt.lechtenberg@tu-dortmund.de

$d_{e/o,\sigma} = \frac{1}{\sqrt{2}}(d_{1,\sigma} \pm d_{2,\sigma})$  for the impurity degrees of freedom [7,18–20,37–40]. In this basis, the orbitals with even/odd parity couple to corresponding even/odd parity conduction bands via the energy- and distance-dependent hybridization functions (see Supplemental Material [41]),

$$\Gamma_e(\epsilon, \vec{R}) = \frac{2\pi V^2}{N} \sum_{\vec{k}} \delta(\epsilon - \epsilon(\vec{k})) \cos^2\left(\frac{\vec{k}\vec{R}}{2}\right), \quad (3a)$$

$$\Gamma_o(\epsilon, \vec{R}) = \frac{2\pi V^2}{N} \sum_{\vec{k}} \delta(\epsilon - \epsilon(\vec{k})) \sin^2\left(\frac{\vec{k}\vec{R}}{2}\right). \quad (3b)$$

A proper consideration of the energy dependence of these functions generally breaks particle-hole symmetry [20,21] and hence destroys the well-known QCP predicted by Jones and Varma [18,19,38].

*Hybridization functions.* Examining the definitions of the hybridization functions  $\Gamma_{e/o}(\epsilon, \vec{R})$  reveals an important fundamental property: If all wave vectors  $\vec{k}'$  fulfilling  $\epsilon(\vec{k}') = 0$  also satisfy the condition  $\vec{k}'\vec{R}_n = \pi n$ , with  $n$  being an integer, one of the two hybridization functions exhibits a pseudogap  $\propto |\epsilon|^2$  because either the sine or the cosine in Eqs. (3) vanishes for  $\epsilon \rightarrow 0$ . While for a general dispersion this requirement is not fulfilled, infinitely many equidistant  $R_n = |\vec{R}_n|$  obeying this requirement are found for a 1D inversion symmetric dispersion with  $\epsilon(k) = \epsilon(|k|)$ . Note that the presented results are valid for the case that the mean free path of the electrons in the conduction channel is larger than the distance  $R$ .

Since the Kondo screening breaks down for a pseudogap hybridization function vanishing as  $|\epsilon|^r$ , with  $r > 1/2$  [42–45], the Kondo effect of the even or odd conduction band will disappear for the specific distances  $k'R_n = \pi n$ , leading to an underscreened spin-1 Kondo fixed point (USK FP) with an effective free spin-1/2 remaining.

The odd-hybridization function completely vanishes for any dispersion and  $R \rightarrow 0$  on all energy scales, leading to a single-channel model and, thus, trivially to an USK FP. For a 1D linear dispersion  $\epsilon(k) = v_F(|k| - k_F)$ , Eqs. (3) yield [39,40]

$$\Gamma_{e/o}^{1D}(\epsilon, R) = \Gamma_0 \left\{ 1 \pm \cos \left[ k_F R \left( 1 + \frac{\epsilon}{D} \right) \right] \right\}, \quad (4)$$

with  $\Gamma_0 = \pi \rho_0 V^2$ , the half bandwidth  $D$ , the constant density of states of the original conduction band  $\rho_0 = 1/2D$ ,  $k_F = \pi/2a$ , and  $a$  the lattice constant. The hybridization function of the even conduction band exhibits a gap for distances  $k_F R = (2n + 1)\pi$  and the one of the odd band for  $k_F R = 2n\pi$ . Note that with increasing distance  $R$ , the frequency of the oscillations in  $\Gamma_{e/o}^{1D}(\epsilon, R)$  increases and, consequently, the width of the gap becomes smaller so that the stable low-energy FP is reached at increasingly lower temperatures.

*Doublet ground state.* Generically, a singlet ground state is found in the TIAM since either the two impurity spins are bound in a local singlet for strong antiferromagnetic correlations between the impurities or the impurity spins are screened by the surrounding conduction band electrons to spatially extended Kondo singlets [18,19,38]. A different situation arises for the specific distances  $k_F R_n = n\pi$ , where one conduction band decouples at low energies. This is

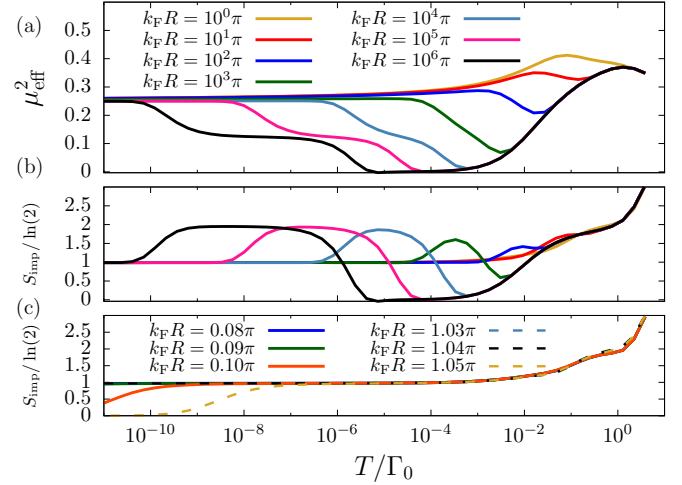


FIG. 1. (a) The effective local magnetic moment  $\mu_{\text{eff}}^2$  and (b) entropy of the impurities for the TIAM plotted against the temperature  $T$  for different distances. (c) The temperature-dependent entropy for distances that slightly deviate from  $R_n = 0$  (solid lines) and  $R_n = 1$  (dashed lines). Model parameters are  $t = 0$ ,  $E = -5\Gamma_0$ ,  $U = 10\Gamma_0$ , and  $D = 10\Gamma_0$ .

demonstrated in Fig. 1 where the effective impurity magnetic moment  $\mu_{\text{eff}}^2$  and the entropy  $S_{\text{imp}}$  [46] are plotted for different  $R_n$ . The USK FP with a free unquenched spin-1/2 remaining is the only stable fixed point for vanishing spin-spin interaction  $K = 0$  ( $t = 0$ ) characterized by  $\mu_{\text{eff}}^2 = 0.25$  and the impurity entropy  $S_{\text{imp}} = \ln(2)$ .

At very large distances  $R_n$ , the gap in one of the hybridization functions becomes very narrow so that the crossover to the USK FP only occurs at very low temperatures. For such distances, at first both impurities are screened by the two conduction bands, leading to an almost vanishing magnetic moment  $\mu_{\text{eff}}^2 \approx 0$  and entropy  $S \approx 0$ . However, the renormalization of the effective Kondo coupling and consequently the screening of one local spin always stops at a finite temperature due to the pseudogap hybridization function and, therefore, the screening is never complete. Since the hybridization to one conduction band vanishes at the Fermi energy, the coupling to that band subsequently decreases until finally the USK FP emerges at very low temperatures.

In between these two FPs, the model exhibits another unstable FP with  $\mu_{\text{eff}}^2 = 0.125$  and entropy  $S_{\text{imp}} = 2\ln(2)$ . The values for  $\mu_{\text{eff}}^2$  and  $S$  are a feature of the gapped Wilson chain [47] and are not related to the impurity physics. While  $\mu_{\text{eff}}^2(T)$  starts to increase until it reaches the value  $\mu_{\text{eff}}^2 = 0.125$  in the regime of the unstable FP, the impurity spins remain screened so that the local moment of the impurities  $\mu_{\text{loc}}^2(T) = T \lim_{h_z \rightarrow 0} \langle S_i^z \rangle / h_z$  [43,48] continues to decrease linearly with decreasing  $T$ . Since the impurity spins are only completely screened at  $T = 0$  in the conventional Kondo problem, the screening of the impurity spins progresses until the USK FP is reached at low temperatures where the local moment  $\mu_{\text{loc}}^2(T)$  and remains constant for  $T \rightarrow 0$  as it is expected for a free but strongly reduced magnetic moment in the Curie-Weiss law [49].

The low-temperature crossover scale from the unstable FP to the stable USK FP depends on the degree of screening:

the smaller  $\mu_{\text{loc}}^2(T_{\text{Gap}})$  at the energy scale  $T_{\text{Gap}}$  at which the pseudogap develops, the smaller the crossover temperature scale. Such a vigorous screening can be achieved in two ways: either the distance  $R_n$  is increased so that the screening stops at lower temperatures (shown in Fig. 1) or the coupling  $V$  to the bands is increased so that the impurities are already strongly screened at a higher  $T$ .

Although a small departure from the specific distances  $R_n$  theoretically always leads to a singlet ground state at very low temperatures, the system will stay in the now unstable doublet fixed point for all experimentally relevant temperatures if the departure is not too large, which can be seen in Fig. 1(c). As a result, using  $k_F = \pi/(2a)$  of a linear dispersion yields that in experiments at finite temperatures, variances of  $R_n$  by up to 20% of the lattice constant are still sufficient to detect a sharp change in the magnetic properties of the system.

**Quantum critical point.** While for a vanishing spin-spin interaction between the impurities the ground state is always a doublet at  $R_n$ , both impurity spins form a local spin singlet for sufficiently strong antiferromagnetic interactions  $K$ . Therefore, these two phases must be separated by a QCP. Unlike the unstable Jones-Varma QCP [18–20] separating two singlet ground states, this QCP is protected by the spin as a conserved quantum number. While the Jones-Varma QPT is continuous [19,20], we found in the parity-symmetric case a linear decreasing energy scale with decreasing  $|t - t_c|$  typical for a parity-protected level-crossing QPT, while in the parity-broken case we observed an exponentially vanishing energy scale indicating a Kosterlitz-Thouless QPT [23,50–52].

The different nature of the QPTs is also revealed in the local correlation function  $\langle \vec{S}_1 \vec{S}_2 \rangle$ . While in the absence of  $K$  ( $t = 0$ ) a local triplet screened by the Kondo effect at low  $T$  to a doublet is part of the ground state, a local singlet forms and suppresses the Kondo effect [18,19] for large antiferromagnetic  $K$ . This leads to  $\langle \vec{S}_1 \vec{S}_2 \rangle > 0$  in the former regime, while in the latter, one finds  $\langle \vec{S}_1 \vec{S}_2 \rangle < 0$ . For the Jones-Varma QCP,  $\langle \vec{S}_1 \vec{S}_2 \rangle$  varies continuously across the QPT and only its derivative diverges at the QCP. This is due to a mixing term in the Hamiltonian [17–19] exchanging even and odd conduction electrons via impurity scattering processes. Global parity remains conserved, but local parity on the impurity subsystem is broken. This is contrasted by the behavior of  $\langle \vec{S}_1 \vec{S}_2 \rangle$  at  $R_n$ , as shown in Fig. 2. Since one band decouples at low-energy scales, the band mixing term is suppressed and a dynamical local parity conservation ensures the conservation of  $\langle \vec{S}_1 \vec{S}_2 \rangle$  at low temperatures and prohibits the decay to its equilibrium value after a spin manipulation. Consequently, the correlation function has to change discontinuously at the QCP for a parity-symmetric model [53].

Furthermore, the QPT is even robust against parity breaking: We have added a small  $\Delta E$  to one of the two single-particle levels, i.e.,  $E_1 = E + \Delta E$ , which is one of several ways of breaking the parity. Although the spin-correlation function varies now continuously in the parity-broken case, as depicted in Fig. 2, other quantities such as the magnetic moment  $\mu_{\text{eff}}^2$ , the entropy  $S_{\text{imp}}$  (shown in the inset of Fig. 2), or the spectral functions still show a discontinuity at the renormalized critical tunneling  $t_c(\Delta E)$ , marked on the  $x$  axis in Fig. 2.

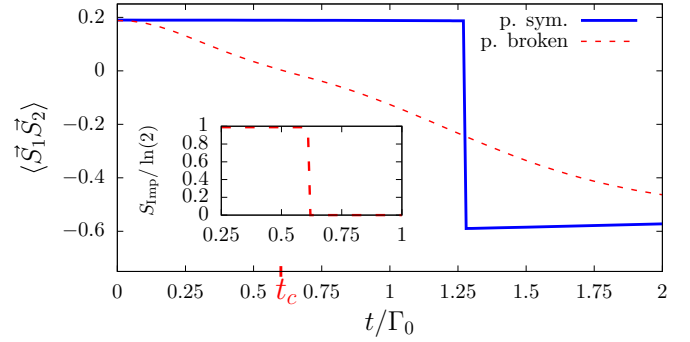


FIG. 2. The correlation function  $\langle \vec{S}_1 \vec{S}_2 \rangle$  plotted against the tunneling  $t$  for the distance  $k_F R = \pi$ . While in the parity-symmetric cases (solid lines)  $\langle \vec{S}_1 \vec{S}_2 \rangle$  must change discontinuously, in the parity-broken case the correlation function is continuous. The inset shows the entropy for the parity-broken case and the new critical  $t_c(\Delta E)$  is marked on the  $x$  axis.

For the parity-conserving case, the spectra of the odd and even orbital [54,55] are shown in Fig. 3 for the two different phases and the distance  $k_F R = \pi$ , at which the even orbital decouples from the conduction band at low-energy scales. The spectral functions exhibit the same features as in the  $R = 0$  case [7,24], but with the role of even and odd spectra interchanged.

The spectrum for the odd orbital develops an underscreened Kondo peak [56] at  $\omega = 0$  for  $t < t_c$ , which collapses once the tunneling exceeds  $t > t_c$ . In this phase, both impurity spins are bound into a local singlet.

In contrast,  $\rho_{\text{even}}$  always develops a gap around the Fermi energy for all  $t \neq t_c$ : the pseudogap in the even-hybridization function suppresses the Kondo screening of the spin in the even orbital. Furthermore, at low frequencies, the orbital decouples from the hybridization processes. Injecting/ejecting an electron into/from the even orbital changes the local particle number, which cannot relax but induces a suddenly changed Coulomb potential for the odd orbital. The only way the system

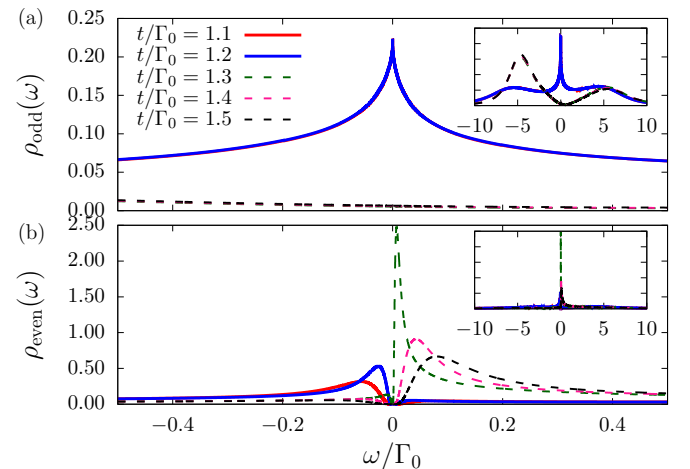


FIG. 3. Spectral function of the (a) odd and (b) even orbital for tunnelings  $t < t_c$  (solid lines) and  $t > t_c$  (dashed lines) and  $\Delta E = 0$ . For the distance  $k_F R = \pi$ , the even orbital decouples for  $T \rightarrow 0$  from the conduction band.

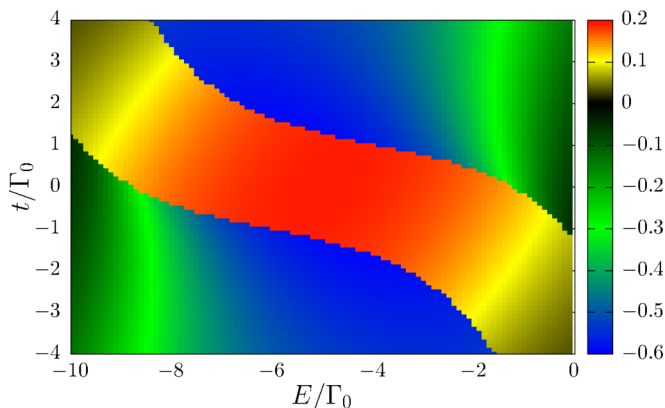


FIG. 4.  $\langle \vec{S}_1 \vec{S}_2 \rangle$  phase diagram plotted against  $E$  and  $t$  for  $k_F R = \pi$  and  $U = 10\Gamma_0$ .

can respond at  $T = 0$  is by changing the many-body ground state. This leads to the well-understood x-ray edge physics [57] also found in the Falicov-Kimball model [58]. The excitations around the Fermi energy thus indicate transitions from the doublet to the singlet phase for  $t < t_c$ , and vice versa for  $t > t_c$ . Consequently, the width of the gap in the spectrum is given by the energy difference between the doublet and singlet state and vanishes for  $t \rightarrow t_c$ . Note that for distances  $k_F R = 2n\pi$ , the spectral functions of the even and odd are interchanged.

In the general parity-broken case, features of the even orbital are weakly mixed into the spectral function of the odd orbital, and vice versa, since in this case both orbitals are coupled to both conduction bands [7]. Experimentally, the QPT can be detected by measuring the differential conductance though an impurity which is proportional to a superposition of the even and odd spectral functions. We predict that for  $t < t_c$ , a clear Kondo peak at the Fermi energy is visible below the Kondo temperature  $T_K$ . This Kondo peak disappears for  $t > t_c$ , and only the finite frequency excitations stemming from the x-ray edge physics of the weakly coupled orbital are mixed in as recently detected in a molecular dimer system [7].

Since the tunneling  $t$  is generated by the overlap of orbital wave functions of the adatoms or molecules in experiment [7], variation of the tunneling  $t$  is experimentally difficult. The case of a fixed  $E$  but different discrete  $t$  changed via molecule geometry has been recently realized [7] for the extreme case of  $R \approx 0$ , but is not suitable for electronic switching of the local spin configuration.

However, it is also possible to evoke the QPT for a fixed tunneling  $t$  via a gate voltage shifting both orbital level energies

$E$ . Figure 4 depicts a phase diagram of the correlation function  $\langle \vec{S}_1 \vec{S}_2 \rangle$  as a function of  $E$  and  $t$ . Ferromagnetic correlations (red and yellow), indicating that the system is in the doublet phase, are developing inside a tube. If either the tunneling  $t$  or the energy level  $E$  is sufficiently increased or decreased, the system is found in the singlet phase (blue and green). Inside the tube, the local magnetic moment and the impurity entropy take the fixed values  $\mu_{\text{eff}}^2 = 0.25$  and  $S_{\text{imp}} = \ln(2)$ , while outside both vanish [59]. For very large positive or negative level energies,  $|\langle \vec{S}_1 \vec{S}_2 \rangle| \rightarrow 0$  decreases continuously since the orbitals become either doubly occupied or empty. Note that in this case, the Kondo effect will also break down in the doublet phase since there is no local moment in the coupled orbital that can be screened. To understand the asymmetry with respect to  $E$  and  $t$ , it is useful to monitor the single-particle energies in the even-/odd-parity basis where both energies are split by the tunneling  $E_{e/o} = E \pm t/2$  so that the even/odd level energy is increased/decreased with increasing  $t$ . In order to evoke a transition from the singlet to the doublet phase, the decoupled orbital has to be shifted towards half filling such that it becomes singly occupied, again which can only happen discontinuously. Consequently, if the distance is changed from an odd distance  $k_F R/\pi = 2n + 1$ , shown in Fig. 4, to an even distance, the roles of the even/odd orbital as the uncoupled/coupled orbital are interchanged and the phase diagram is hence mirrored at the line  $t = 0$ .

*Summary.* We have shown that the TIAM exhibit a QCP for a 1D dispersion  $\epsilon(k) = \epsilon(|k|)$  in the cases that the impurities are separated by specific distances  $R_n$ . In contrast to the unstable QCP [18,19] usually discussed in the context of the two-impurity models, the QCP presented in this Rapid Communication is stable to departure from particle-hole and parity symmetry.

We believe that this system may be of great relevance for spintronic devices since it is possible by applying gate voltages to turn on and off a free magnetic moment which is not screened at low temperatures. Along with the magnetic moment, one can switch on and off a Kondo effect with its sharp conductance peak at the Fermi energy. Furthermore, in the parity-symmetric case, the spin-spin correlation between both impurity spins is protected by the parity as a conserved quantity, making this system promising for spin-qubit realizations.

*Acknowledgments.* We acknowledge useful discussions with S. F. Tautz and R. Bulla. B.L. thanks the Japan Society for the Promotion of Science (JSPS) and the Alexander von Humboldt Foundation.

- 
- [1] I. Žutić, J. Fabian, and S. Das Sarma, *Rev. Mod. Phys.* **76**, 323 (2004).
- [2] M. Misiorny, M. Hell, and M. R. Wegewijs, *Nat. Phys.* **9**, 801 (2013).
- [3] W. Han, R. K. Kawakami, M. Gmitra, and J. Fabian, *Nat. Nano* **9**, 794 (2014).
- [4] H. Jöhl, M. D. K. Lee, S. P. N. Ng, H. C. Kang, and E. S. Tok, *Sci. Rep.* **4**, 7594 (2014).
- [5] O. V. Yazyev and L. Helm, *Phys. Rev. B* **75**, 125408 (2007).
- [6] J. Bork, Y.-h. Zhang, L. Diekhoner, L. Borda, P. Simon, J. Kroha, P. Wahl, and K. Kern, *Nat. Phys.* **7**, 901 (2011).
- [7] T. Esat, B. Lechtenberg, T. Deilmann, C. Wagner, P. Krüger, R. Temirov, M. Röhlfing, F. B. Anders, and F. S. Tautz, *Nat. Phys.* **12**, 867 (2016).
- [8] N. Atodiresei, J. Brede, P. Lazić, V. Caciuc, G. Hoffmann, R. Wiesendanger, and S. Blügel, *Phys. Rev. Lett.* **105**, 066601 (2010).
- [9] L. Bogani and W. Wernsdorfer, *Nat. Mater.* **7**, 179 (2008).
- [10] S. Sanvito, *Chem. Soc. Rev.* **40**, 3336 (2011).

- [11] W. J. M. Naber, S. Faez, and W. G. van der Wiel, *J. Phys. D* **40**, R205 (2007).
- [12] V. A. Dediu, L. E. Hueso, I. Bergenti, and C. Taliani, *Nat. Mater.* **8**, 707 (2009).
- [13] A. J. Drew, J. Hoppler, L. Schulz, F. L. Pratt, P. Desai, P. Shakya, T. Kreouzis, W. P. Gillin, A. Suter, N. A. Morley, V. K. Malik, A. Dubroka, K. W. Kim, H. Bouyanfif, F. Bourqui, C. Bernhard, R. Scheuermann, G. J. Nieuwenhuys, T. Prokscha, and E. Morenzoni, *Nat. Mater.* **8**, 109 (2009).
- [14] A. Spinelli, M. Gerrits, R. Toskovic, B. Bryant, M. Ternes, and A. F. Otte, *Nat. Commun.* **6**, 10046 (2015).
- [15] S. Doniach, *Physica B (Amsterdam)* **91**, 231 (1977).
- [16] T. Jabben, N. Grewe, and S. Schmitt, *Phys. Rev. B* **85**, 165122 (2012).
- [17] O. Sakai and Y. Shimizu, *J. Phys. Soc. Jpn.* **61**, 2333 (1992).
- [18] B. A. Jones, C. M. Varma, and J. W. Wilkins, *Phys. Rev. Lett.* **61**, 125 (1988).
- [19] B. A. Jones and C. M. Varma, *Phys. Rev. B* **40**, 324 (1989).
- [20] I. Affleck, A. W. W. Ludwig, and B. A. Jones, *Phys. Rev. B* **52**, 9528 (1995).
- [21] R. M. Fye, *Phys. Rev. Lett.* **72**, 916 (1994).
- [22] The USK FP differs from the strong-coupling fixed point usually discussed in the context of an underscreened Kondo effect by an additional free conduction band with zero phase shift.
- [23] M. Vojta, R. Bulla, and W. Hofstetter, *Phys. Rev. B* **65**, 140405 (2002).
- [24] S. Nishimoto, T. Pruschke, and R. M. Noack, *J. Phys.: Condens. Matter* **18**, 981 (2006).
- [25] M. A. Blachly and N. Giordano, *Phys. Rev. B* **46**, 2951 (1992).
- [26] J. F. DiTusa, K. Lin, M. Park, M. S. Isaacson, and J. M. Parpia, *Phys. Rev. Lett.* **68**, 678 (1992).
- [27] M. A. Blachly and N. Giordano, *Phys. Rev. B* **51**, 12537 (1995).
- [28] P. Mohanty and R. A. Webb, *Phys. Rev. Lett.* **84**, 4481 (2000).
- [29] H. Masai, J. Terao, S. Seki, S. Nakashima, M. Kiguchi, K. Okoshi, T. Fujihara, and Y. Tsuji, *J. Am. Chem. Soc.* **136**, 1742 (2014).
- [30] A. V. Gorshkov, M. Hermele, V. Gurarie, C. Xu, P. S. Julienne, J. Ye, P. Zoller, E. Demler, M. D. Lukin, and A. M. Rey, *Nat. Phys.* **6**, 289 (2010).
- [31] L.-M. Duan, *Europhys. Lett.* **67**, 721 (2004).
- [32] B. Paredes, C. Tejedor, and J. I. Cirac, *Phys. Rev. A* **71**, 063608 (2005).
- [33] K. G. Wilson, *Rev. Mod. Phys.* **47**, 773 (1975).
- [34] H. R. Krishna-murthy, J. W. Wilkins, and K. G. Wilson, *Phys. Rev. B* **21**, 1003 (1980).
- [35] H. R. Krishna-murthy, J. W. Wilkins, and K. G. Wilson, *Phys. Rev. B* **21**, 1044 (1980).
- [36] R. Bulla, T. A. Costi, and T. Pruschke, *Rev. Mod. Phys.* **80**, 395 (2008).
- [37] C. Jayaprakash, H. R. Krishna-murthy, and J. W. Wilkins, *Phys. Rev. Lett.* **47**, 737 (1981).
- [38] B. A. Jones and C. M. Varma, *Phys. Rev. Lett.* **58**, 843 (1987).
- [39] L. Borda, *Phys. Rev. B* **75**, 041307 (2007).
- [40] B. Lechtenberg and F. B. Anders, *Phys. Rev. B* **90**, 045117 (2014).
- [41] See Supplemental Material at <http://link.aps.org/supplemental/10.1103/PhysRevB.96.041109> for a detailed description of the mapping to the parity basis.
- [42] R. Bulla, T. Pruschke, and A. C. Hewson, *J. Phys.: Condens. Matter* **9**, 10463 (1997).
- [43] C. Gonzalez-Buxton and K. Ingersent, *Phys. Rev. B* **57**, 14254 (1998).
- [44] K. Chen and C. Jayaprakash, *J. Phys.: Condens. Matter* **7**, L491 (1995).
- [45] K. Ingersent, *Phys. Rev. B* **54**, 11936 (1996).
- [46] Both quantities  $\mu_{\text{eff}}^2$  and  $S_{\text{imp}}$  are calculated as usual in the NRG via  $A(T) = A_{\text{tot}}(T) - A_{\text{free}}(T)$ , where  $A_{\text{tot}}(T)$  is the measured quantity of the total system, consisting of the impurities coupled to the bath. From this, the quantity of a reference system, i.e., one without impurities, is subtracted.
- [47] More details on the origin of this unstable fixed point can be found in the Supplemental Material [41].
- [48] T. Chowdhury and K. Ingersent, *Phys. Rev. B* **91**, 035118 (2015).
- [49] The temperature-dependent behavior of  $\mu_{\text{loc}}^2(T)$  is depicted in the Supplemental Material [41].
- [50] A. K. Mitchell, T. F. Jarrold, M. R. Galpin, and D. E. Logan, *J. Phys. Chem. B* **117**, 12777 (2013).
- [51] A. K. Mitchell, T. F. Jarrold, and D. E. Logan, *Phys. Rev. B* **79**, 085124 (2009).
- [52] W. Hofstetter and H. Schoeller, *Phys. Rev. Lett.* **88**, 016803 (2001).
- [53] For a more detailed explanation of the origin of the discontinuity, we refer the reader to the Supplemental Material [41], which includes Refs. [60–62].
- [54] R. Peters, T. Pruschke, and F. B. Anders, *Phys. Rev. B* **74**, 245114 (2006).
- [55] A. Weichselbaum and J. von Delft, *Phys. Rev. Lett.* **99**, 076402 (2007).
- [56] N. Roch, S. Florens, T. A. Costi, W. Wernsdorfer, and F. Balestro, *Phys. Rev. Lett.* **103**, 197202 (2009).
- [57] B. Roulet, J. Gavoret, and Nozières, *Phys. Rev.* **178**, 1072 (1969); N. P. and C. T. de Dominicis, *ibid.* **178**, 1097 (1969).
- [58] Q. Si, G. Kotliar, and A. Georges, *Phys. Rev. B* **46**, 1261 (1992); F. B. Anders and G. Czycholl, *ibid.* **71**, 125101 (2005).
- [59] The phase diagrams of  $\mu_{\text{eff}}^2$  and  $S_{\text{imp}}$  are shown in the Supplemental Material [41].
- [60] M. R. Galpin, D. E. Logan, and H. R. Krishnamurthy, *Phys. Rev. Lett.* **94**, 186406 (2005).
- [61] J. R. Schrieffer and P. A. Wolff, *Phys. Rev.* **149**, 491 (1966).
- [62] R. Žitko and J. Bonča, *Phys. Rev. B* **74**, 045312 (2006).